Ab Initio Study of the Activation of Ammonia by Co^+

M. Hendrickx,* M. Ceulemans, K. Gong, and L. Vanquickenborne

Department of Chemistry, University of Leuven, Celestijnenlaan 200F, B-3001 Heverlee-Leuven, Belgium

Received: May 14, 1997; In Final Form: July 16, 1997[⊗]

Mechanistic aspects of the reaction of Co^+ with ammonia are investigated by ab initio calculations. The potential energy surface is explored at the CASSCF level. Relative stabilities of the various stationary points on the reaction path are obtained by applying the CASPT2 technique. Binding energies for the reaction products $CoNH_3^+$, $CoNH_2^+$, and CoH^+ are calculated to be 52.1, 66.7, and 51.5 kcal/mol, respectively. They correspond reasonably well with the relevant experimental values of 58.8 ± 5, 61.3 ± 2, and 46.6 ± 2 kcal/mol, respectively, falling just a few kcal/mol outside the error bars of the measurements. The $HCoNH_2^+$ isomer of the $CoNH_3^+$ adduct is confirmed to represent a local minimum on the potential energy surface. It is separated from the adduct by an energy barrier of 15 kcal/mol, and its formation from the reactants is just slightly exothermic by a few kcal/mol. The H_2 elimination is experimentally not observed as a consequence of a complex tight four center transition state at about 58 kcal/mol above the ground state asymptote. The $CoNH_2^+$ and CoH^+ exit channels are energetically situated below this barrier. Due to the high threshold energy, both reaction products are formed directly by simple N−H bond fission without $HCoNH_2^+$ acting as an intermediate.

Introduction

In the past decade reactions of single-charged transition metal cations of the first row with small organic and inorganic molecules have been a subject of considerable interest.[1,2] Especially, the reactions of small hydrocarbons have been the focus of attention during the past few years.[3,4] Theoretical calculations turned out to be essential to unravel the underlying reaction mechanism of the different observed elimination channels. At present all available data point[5−12] to the fact that the insertion products HMR^+ for the late first row transition metal cations Fe^+ and Co^+ do not exist. Early cations (Sc^+, V^+, and Ti^+), on the contrary, can react in a stepwise fashion, where the oxidative insertion into a C−H bond is predicted to be the first step. In agreement with this conclusion, a previous theoretical study has indeed found that only for the early transition metal cations do the relevant hydridoalkyl complexes HMR^+ represent a sufficiently stable minimum on the potential energy surface.[13] The experimental evidence for the existence of this type of species on the other hand is largely circumstantial.[14−16]

The situation is quite different for the reactions of metal cations with small nonhydrocarbon molecules. Indeed, for the insertions into X−H bonds (X = O, N), there are indications in favor of stable insertion complexes also for the late transition metal cations.[17−19] Since such complexes were recently[13] shown not to exist for hydrocarbons, the study of a wider range of reactions appears to be appropriate. In the present paper we report on the reaction of Co^+ with ammonia. For this reaction detailed experimental data are available in the literature.[20,21] Using guided ion beam experiments, it was possible to identify four species in the mass spectrometer. At low kinetic energies of the Co^+ cation, reactions 1 and 2 are observed. At higher entrance energies (larger than 2 eV), dissociation channels 3 and 4 are beginning to emerge, with the latter one becoming dominant at kinetic energies larger than 3.2 eV. Elimination of H_2, reaction 5, which was observed for the early cations[22,23] Sc^+, Ti^+, and V^+, does not occur for Co^+.

$$Co^+ + NH_3 \rightarrow CoNH_3^+ \quad (1)$$

$$\rightarrow HCoNH_2^+ \quad (2)$$

$$\rightarrow CoNH_2^+ + H \quad (3)$$

$$\rightarrow CoH^+ + NH_2 \quad (4)$$

$$(\rightarrow CoNH^+ + H_2) \quad (5)$$

Only reaction 1 is experimentally found to be exothermic. The reaction product $CoNH_3^+$ is stabilized by secondary collisions, and therefore the cross section of this molecular complex depends on the ammonia pressure. The exothermic nature of reaction 1 is demonstrated by the decrease of the cross section of $CoNH_3^+$ with increasing kinetic energies. In addition, a second feature corresponding to the same molecular mass and that peaks near 1.3 eV is present. Using ND_3 as a reactant shifts this peak by 2 kcal/mol, suggesting that the responsible entity is likely to be the inserted complex $HCoNH_2^+$. On the basis of the relative reaction efficiencies for the formation of CoH^+ and $CoNH_2^+$, the experiments rather surprisingly indicate that reactions 3 and 4 do not proceed via the intermediate $HCoNH_2^+$. With this problem in mind, we carried out ab initio calculations in order to solve the uncertainty as to the existence of the insertion complex. Further on we will pay special attention as to why reaction 5 is not observed experimentally. This is not at all evident, since $CoNH^+$ can be supposed to be rather stable due to the possible presence of a triple bond between Co^+ and NH. Indeed, the low-lying ^5F ($4s^13d^7$) state of this metal cation has the required number of unpaired electrons to form a triple bond with a NH ligand.

Computational Details

The ab initio calculations were performed by the CASPT2[24] multireference technique, in which the reference function is of the CASSCF type. The active spaces used for the different species considered can be found in Table 1 and are denoted as

[⊗] Abstract published in *Advance ACS Abstracts,* October 1, 1997.

S1089-5639(97)01603-4 CCC: $14.00

TABLE 1: Active Spaces Used in the CASSCF Geometry Optimizations (AS1) and in the CASPT2 Calculation of the Thermochemistry (AS2)

complex	AS1		AS2	
$Co^+ + NH_3$	5×3d, 4s	8i6[a]	+ 5×3d′	8i11
$CoNH_3^+$	5×3d, 4s	8i6	+ 5×3d′	8i11
TS1	σ_{CoH}, σ^*_{CoH}, σ_{CoN}, σ^*_{CoN}, 4×3d, $N_{lone\ pair}$	12i9	+ 4×3d′	12i13
$HCoNH_2^+$	σ_{CoH}, σ^*_{CoH}, σ_{CoN}, σ^*_{CoN}, π_{CoN}, π^*_{CoN}, 3×3d	12i9	+ 3×3d′	12i12
CoH^+	σ_{CoH}, σ^*_{CoH}, 5×3d	9i7	+ 5×3d′	9i12
$CoNH_2^+$	σ_{CoN}, σ^*_{CoN}, 5×3d, $N_{lone\ pair}$	11i8	+ 5×3d′	11i13
TS2	σ_{CoH}, σ^*_{CoH}, σ_{CoN}, σ^*_{CoN}, 4×3d $N_{lone\ pair}$, σ_{NH}, σ^*_{NH}	14i11	*b*	14i11
$CoNH^+$	σ_{CoN}, σ^*_{CoN}, 3×3d, $N_{lone\ pair}$, 2×π_{CoN}, 2×π^*_{CoN}	12i9	+ 3×3d′	12i12

[a] *xiy* denotes a complete active space with *x* electrons distributed among *y* orbitals. [b] Cannot be calculated because accounting for the full double shell effect is computationally impossible.

xiy, with *x* the number of electrons and *y* the number of active orbitals. The minimal active space that is obtained by incorporating the metal 3d and 4s orbitals along with the interacting ligand orbitals is denoted as AS1. Similar calculations for the NiH and CuH molecules clearly show[25] that in order to obtain sufficient accurate binding energies, the 3d′ orbitals should also be included in the active space. Due to the important contributions of the $4s^03d^8$ and $4s^13d^7$ configurations in the CASSCF wave function, the inclusion of an extra d-type orbital in the active space substantially improves the results. In this way we account to a significant extent for the important relaxation effects that take place in these orbitals. This is known as the double-shell effect and leads to an active space for the different molecules which is denoted as AS2 in Table 1. With the exception of the AS2 space for TS2 (see below), AS1 and AS2 separately are compatible active spaces for all the structures considered. In all the CASPT2 calculations the AS2 space was used, and only the 1s, 2s, and 2p electrons of Co and the 1s electrons of N were not correlated.

The geometries of the various structures on the potential energy surface are obtained at the CASSCF level, using gradient techniques. No symmetry restrictions were imposed. If a molecule was found to resemble closely a higher symmetry, the geometry was reoptimized within the higher symmetry constraints. For the geometry optimizations the AS1 active space is suited to calculate the geometries on the potential surface. Since the interaction between NH_3 and Co^+ in the adduct is mainly electrostatic, only the metal 3d, 4s (and 3d′) orbitals will be included in the active space. As will be shown for these molecular complexes, reoptimizing the metal−ligand distance at the CASPT2 level increases the bond length significantly. In those cases where the CASSCF treatment is not sufficient, the transition state was located by performing CASPT2 calculations along the reaction path (see below). The reaction path itself is obtained by applying the coordinate-driven method. At several points along the reaction coordinate the molecule is optimized while the reaction-determining parameter is kept fixed. Plotting the CASPT2 energies gives a maximum that corresponds to a transition state.

The basis sets are of the ANO type. The contraction scheme[26] is (17s12p9d 4f)/[6s4p3d1f] for Co, (10s4p3d)/[4p3p1d] for N, and (7s4p)/[3s1p] for H. This basis set has been shown to give good results for this type of reactions.[12] The triple valence segmented basis sets from the GAMESS basis library[27] are used for the transition-state optimizations. To determine the thermochemistry of the reaction surface, the binding energies of the complexes are calculated by using the AS2 active space. The nitrogen hydrogen species are treated on the MP2 level. Although this leads to unbalanced active spaces for some products and reactants, the resulting errors will be shown to be small and will not affect the relative energies of the complexes to any significant extent. Similar considerations have been used in studies on $Cr(CO)_6$.[28] Zero-point vibrational corrections are performed by calculating numerically the frequencies for the stationary structures on the potential energy surface. The basis set superposition error (BSSE) is estimated by using the counterpoise method. Since the 4s occupation varies along the reaction surface, the relativistic mass−velocity corrections and the Darwin terms[40] have to be taken into account. All CASPT2 calculations are performed with the MOLCAS-3 software.[29] Geometry optimizations and transition-state localization are carried out with the GAMESS program.[27]

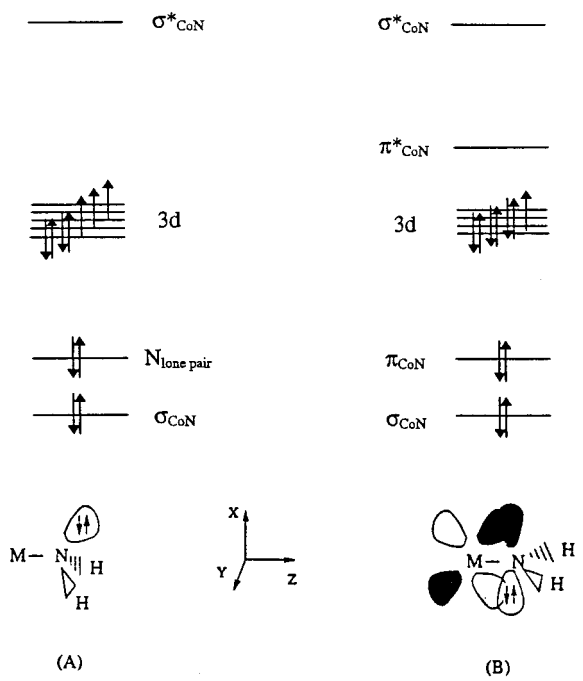

Figure 1. Qualitative molecular orbital diagram for quartet (A) and doublet (B) structure of the $CoNH_2^+$ complex.

Results and Discussion

Exit Channels. To obtain an idea about the accuracy of our calculations, we first examine the reaction products $CoNH_3^+$, $CoNH_2^+$, $CoNH^+$, and CoH^+ of the various exit channels. For all these complexes, with the exception of $CoNH^+$, which was not observed, experimental binding energies can be used to calibrate our level of theory. Sketches of these molecules as well as the schematic representation of the entire reaction mechanism are depicted in Figure 3.

$CoNH_3^+$. Experimental[21] and theoretical[30] studies have shown that molecular complexes (adducts) of metal ions and NH_3 form strong bonds, as opposed to the molecular complexes with methane. Experimentally, $Co^+(^3F)$ is found to coordinate by about 55 kcal/mol to NH_3. The methane Co^+ bond is only 21 kcal/mol, or 2.8 times less.[31] This difference can be understood in terms of ion−dipole interactions; NH_3 has a permanent dipole, whereas methane has only an induced dipole. At the CASSCF level, the geometry of the complex has a C_{3v} symmetry. The ground state turned out to be $^3A_2$, with $(9a_1)^2(4e)^4(5e)^2$ as the leading configuration. At the CASPT2 level, on the contrary, ^3E ($(9a_1)^2(4e)^3(5e)^3$) becomes the ground state. The Jahn−Teller effect was calculated not to cause large energy

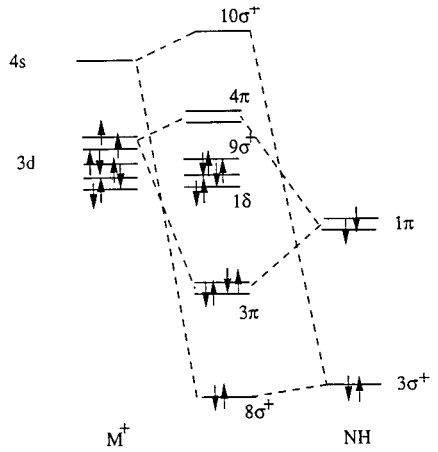

Figure 2. Qualitative molecular orbital diagram for the $CoNH^+$ complex. The depicted orbital occupations correspond to the leading configuration of the $^1\Sigma^+$ state. It shows that the $9\sigma^+$ orbital is below the 4π orbital.

differences. An optimization at the CASSCF level of the $^3A''$ component of the ^3E state resulted in lowering the energy by about 2.5 kcal/mol. In view of this small value we decided the carry out the computationally more demanding CASPT2 calculations by imposing C_{3v} symmetry, a procedure also applied in ref 30. Optimizing at the CASSCF level gives a Co−N bond length of 2.07 Å. Reoptimizing at the CASPT2 level lowers the bond distance by 0.12 Å. The CASPT2 binding energy was calculated to be 57.0 kcal/mol. Correcting this value for the BSSE (5.5 kcal/mol) and relativistic corrections (3.5 kcal/mol) results in a D_e of 55.0 kcal/mol, which is in good agreement with the MCPF value of 53.2 kcal/mol calculated by Langhoff et al.[30] A zero-point vibrational correction lowers our theoretical binding energy by 2.9 kcal/mol to 52.1 kcal/mol. This is a slight underestimation of the experiment (58 ± 5 kcal/mol).[21]

$CoNH_2^+$. For the metal amide ions the bond strengths are experimentally known to be between 10 and 40 kcal/mol stronger than their methyl analogues.[2] On the basis of theoretical calculations carried out on the complexes MNH_2^+ (M = Sc to Cr) by Mavridis et al.[32] and Kappelos et al.,[33] Clemmer et al.[21] made a proposition for the electronic structure of $CoNH_2^+$. The corresponding molecular orbital diagram as well as drawings that illustrate the major orbital interactions between the Co^+ cation and the NH_2 ligand are shown in Figure 1. Two types of interactions are expected by these authors to be possible. In the first type, a double bond between the metal and the ligand is formed, which implies an sp^2 hybridization of nitrogen and results in a planar structure for the molecule. The unbound sp^2 orbital of this atom interacts with the 4s orbital of the metal and produces a σ bond. The remaining doubly occupied p orbital of N forms a π bond with a d_π orbital. The remaining unaffected metal d orbitals constitute in the molecular orbital diagram a cluster of four nonbonding d orbitals. In a second type of bonding, the NH_2 ligand is sp^3 hybridized, and it therefore coordinates to the metal cation in the same way as its isoelectronic methyl counterpart. One of the two free sp^3 orbitals forms a covalent σ bond with the 4s metal orbital. The other free sp^3 orbital, which is doubly occupied, does not participate in the bonding process and becomes a lone pair in the $CoNH_2^+$ complex. As a consequence, the whole 3d shell stays largely intact. The main difference between these two binding types is the resulting spin multiplicity and the equilibrium geometry of the $CoNH_2^+$ complex. A low spin (doublet) corresponds to a double bond and a planar structure. A high spin (quartet), on the contrary, results from the absence of a π interaction and gives a bent structure. Both possibilities were investigated. The geometries and energetics are shown in Table 2.

The low-spin complexes all converge to a C_{2v} geometry. Consequently, we need to consider four states as possible candidates for the ground states; $^2A_1$, $^2A_2$, $^2B_1$ and $^2B_2$. The ground state is $^2A_1$, with the other states only situated about 3 kcal/mol higher. In accordance with the theoretical model of Clemmer et al.[21] a double bond between the N and the Co is clearly found. The quartet states (high-spin) converge to a bent C_s geometry, with a $^4A'$ as the lowest state. A $^4A''$ state is situated merely about 1 kcal/mol higher in energy. This confirms the almost intact atomic 3d manifold in the sense that excitations in such a manifold do not change the energy much. Both high-spin states possess a sp^3 lone pair on nitrogen. The binding energies (Table 2) show that $^4A'$ is the ground state, with a D_e value of 69.8 kcal/mol and a D_0 of 66.7 kcal/mol. The low-spin complex has a D_e value of 54.2 kcal/mol and a D_0 value of 52.0 kcal/mol, which places it about 15 kcal/mol above the quartet ground state. The calculated binding energy of $CoNH_2^+$ is in reasonable agreement with the experimental value of 61 ± 2 kcal/mol.[21]

By way of contrast, the early cations of the first-row transition metals have a C_{2v} ground-state conformation.[32,33] We believe that this difference with the bent structure for the ground state of $CoNH_2^+$ is the outcome of the increased shielding effect of the 4s orbital of Co^+ that diminishes the capability of the 3d orbitals to interact with the NH_2 ligand. For the early metal cations, this shielding effect is believed to be smaller, which permits the d_π orbital to play a more important role in the binding process. Although a similar conclusion was reached in the previous theoretical study of the $HMCH_3^+$ complexes (M = Sc−Cu), additional calculations on MNH_2^+ for all cations of the first-row transition metal cations are needed to substantiate the proposed trend of the 3d participation in the metal−ligand bonding. This clearly falls outside the scope of the present paper and will be addressed in a subsequent paper. It should however be mentioned that for the early metal cations Sc^+ to Cr^+, a systematic GVB study[33] of the metal amide ions showed a gradual decrease in the binding energies of the low-spin ground states as one goes from Sc^+ to Cr^+. Hence, a high-spin ground state belongs to the possibilities.

$CoNH^+$. MNH^+ (M = Sc, Ti, V, Y, Zr, Nb, La, or Ta)[22,23,34] complexes are experimentally found to have rather large binding energies, which can be explained in terms of the multiple bonding character between the metal and the NH radical. The metal can form up to three bonds with the nitrogen atom, as is illustrated in the MO scheme in Figure 2. This multiple-bonding between the nitrogen and the metal was also characterized in a previous study of the related MNH^+ molecules.[35] Figure 2 shows that the ground state will be determined by splitting the atomic d shell. If this splitting is large, than a closed shell structure will be the ground state. If, on the other hand, this splitting is small, a quintet can emerge as the ground state.

Three spin multiplicities can therefore result from the interaction between Co^+ and NH; a singlet, a triplet, and a quintet. Only the triplet can be formed in a diabatic way, i.e., without a spin flip occurring during the reaction. The singlet and the quintet should however also be considered, since at low kinetic energies an adiabatic reaction process is possible. To allow convergence to a bent structure, all geometry optimizations were started with a Co−N−H angle of 130°. In accordance with previous theoretical calculations on MNH^+ complexes,[35] all the electronic states considered have been found to nearly converge to $C_{\infty v}$, and the CoNH bond angle differs by no more

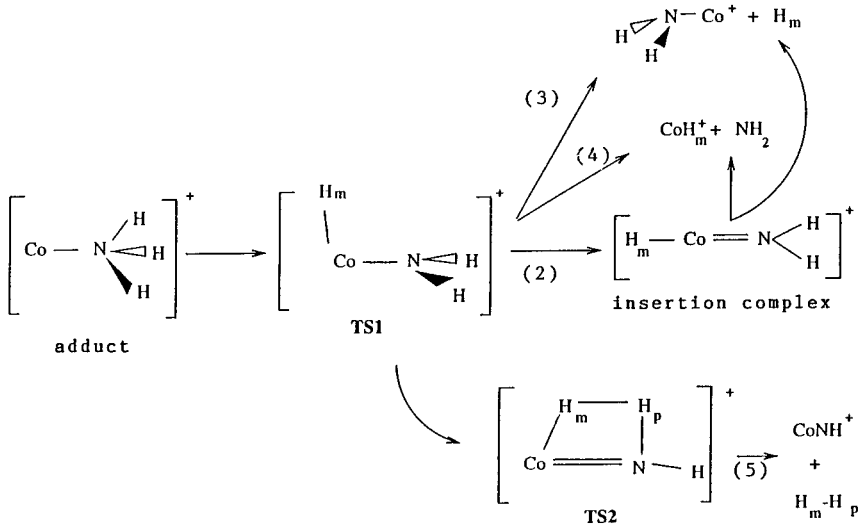

Figure 3. Schematic representation of the mechanism for the reaction of Co^+ with ammonia.

TABLE 2: Geometry and Binding Energies for the $CoNH_2^+$ Complex

	doublets				quartets	
	$^2A_1$	$^2B_1$	$^2B_2$	$^2A_2$	$^4A'$	$^4A''$
Co−N (Å)	1.92	2.13	2.12	2.10	1.86	1.86
∠Co−N−H (deg)	125.9	125.9	125.9	125.8	118.4	118.9
∠H−Co−N−H(deg)	180[a]	180	180	180	135.2	136.8
D_e[b]	54.2	51.7	50.8	50.7	69.8	68.4
D_0[c]	52.0				66.7	
expt[d]					61 ± 2	

[a] Value of 180° corresponds to a planar structure in Figure 1B. [b] CASPT2 (AS2) results incorporating relativistic corrections and basis set superposition error. [c] Zero-point vibrational energies calculated for the lowest doublet and quartet state. [d] Experimental value taken from ref 21.

TABLE 3: Geometries and Bond Dissociation Energies of the $CoNH^+$ Complex

	$^1\Sigma^+$	$^3\Phi$	$^5\Delta$
Co−N (Å)	1.66	1.68	1.72
N−H (Å)	1.01	1.01	1.00
D_e	68.7	64.6	82.3
D_0	66.1	62.0	79.4

[a] Caspt2 (AS2) results incorporating relativistic corrections and basis set super position error.

TABLE 4: Leading Configurations for the Different Spin States of $CoNH^+$

state	$8\sigma^+$	$9\sigma^+$	$10\sigma^+$	3π	4π	1δ	weight (%)
$^1\Sigma^+$	2	2	0	4	0	4	66
$^3\Phi$	2	2	0	4	1	3	73
$^5\Delta$	2	1	0	4	2	3	82

than 3° from linearity. To obtain a good description of the electronic structure involved, the geometries are reoptimized in the $C_{\infty v}$ symmetry. The errors due to the Renner−Teller effect (in the case of degeneracy) are calculated to be less than 3 kcal/mol. The geometries and energetics of the ground states are shown in Table 3. The leading configurations of the ground states of each spin multiplicity are given in Table 4.

Table 3 shows a $^5\Delta$ ground state. This means that the splitting between the mainly nonbonding d orbitals is not large enough to overcome the additional electron repulsion required for pairing two electrons with opposite spin. The calculated binding energy of 79.4 kcal/mol is clearly larger than for $CoNH_2^+$ and CoH^+ (see below). The binding energies of the early metal cation MNH^+ complexes are found to be on the average 20 kcal/mol larger than that for the $CoNH^+$ complex. One can assume for the early metals a strong multiple (intermediate between a double and triple) bond between M^+ and NH, as expected from theoretical considerations.[35] In view of our previous[13] study, the smaller binding energies for $CoNH^+$ can be explained by the trend of the radial extent of the radius of the 3d orbital across the row. For the late metal cations, the 3d orbital is more contracted, which results in a weaker π interaction.

CoH^+. Theoretical studies of the metal hydride ions are already performed at the GVB−CI level by Schilling et al.[36] and at the MCPF level by Petterson et al.[37] Both previous theoretical studies find the CoH^+ binding energy to be about 45 kcal/mol. Our CASPT2 calculations confirm the ground-state $^4\Phi$ obtained by Schilling et al. and Petterson et al. The leading configuration is $6\sigma^2 7\sigma^2 3\pi^3 1\delta^3$. The Co−H distance at the CASSCF level is 1.63 Å, in good agreement with the GVB−CI value (1.61 Å) and somewhat larger than the MCPF value (1.54 Å). Our calculated Co−H stretching frequency amounts to 1608 cm^{-1}, which compares very well with the GVB−CI frequency of ref 36 (1631 cm^{-1}). The MCPF value of 1888 cm^{-1} obtained for this complex differs by more than 200 cm^{-1} from these values. We can conclude that the two multireference methods (CASSCF and GVB−CI) give very similar results for the bond distance and the stretching frequency, whereas the single-reference MCPF method predicts a shorter bond distance and a higher frequency. After correcting for BSSE (2.5 kcal/mol), relativistic effects (8.5 kcal/mol), and zero-point vibrational energies, our binding energy amounts to 51.1 kcal/mol. The experimental values corresponds to 46.6 ± 2 kcal/mol.[38] Our calculated binding energies slightly overestimate the experimental value, in contrast with both earlier theoretical calculations.

Reaction Mechanism for $Co^+ + NH_3$. A comparison of the calculated binding energies with the corresponding experimental values shows that our level of approximation used to describe the electronic structure of the different molecules is adequate to give a reasonable picture of the potential energy surface. Indeed, for $CoNH_2^+$ and CoH^+ our calculations only slightly overestimate the experimental binding energies by about 5 kcal/mol. The origin of this deviation must be sought in the partial occupation of the 4s orbital in these complexes. As the binding energies are calculated with respect to the ^3F ($4s^0 3d^8$) ground-state asymptote of Co^+, any error present in the calculation of the atomic ^3F ($4s^0 3d^8$) → ^5F ($4s^1 3d^7$) transition

TABLE 5: Geometries for the Transition State TS1 (H_m Denotes the Migrating Proton)

	CASSCF[a]	CASPT2[b]
$\angle H_m-Co-N$ (deg)	56.6	104.0
Co−N (Å)	1.83	2.09
$Co-H_m$ (Å)	1.61	1.64
$\angle H_m-Co-N-H$ (deg)	73.2	74.7
∠Co−N−H (deg)	123.5	125.8

[a] Localized at the CASSCF level. [b] Transition state localized by performing CASPT2 calculations on the CASSCF reaction path.

is likely also to be present in the binding energies. Using the same basis set and the AS2 active space, the CASPT2 $^3F \rightarrow {}^5F$ excitation energy, corrected for relativistic effects, amounts to 2.5 kcal/mol. Due to the larger dynamic correlation present in the d^8 ground state, our calculations underestimate the experimental excitation energy (10 kcal/mol *J*-averaged value) by 7.5 kcal/mol. This shortcoming is quite common and well-known in transition metal chemistry.[39] To avoid this type of error, large basis sets in combination with extensive correlation treatment are necessary. Such calculations are not feasible for the complexes studied in the present paper. Since the 4s occupation does not vary much across the potential energy surface, the relative energies of the different equilibrium structures and transition states can be expected to have a much smaller error so as to make the results more reliable.

Intermediates and Transition States. Oxidative Addition: TS1. The first step in the reaction is the formation of the adduct. In this complex ion one NH bond is activated and an insertion in this bond is realized. This activation process involves a first transition state: TS1. A survey at the CASSCF level of the potential energy surface results in a $^3A'$ transition state at a H−Co−N angle of 53.8°, possessing a C_s symmetry and one imaginary frequency of 1024i cm^{-1}. However, the CASPT2 energy calculated for this CASSCF transition state is 2 kcal/mol below the $HCoNH_2^+$ insertion complex. The problem arises from the poor description of the dynamic correlation at the CASSCF level, stabilizing the s^1d^7 electronic structure of the $HCoNH_2^+$ insertion complex, with respect to the predominant d^8 character of the TS1. It is interesting to note that the insertion of Co^+ into a CH bond gave a similar problem. However, a transition-state search along the reaction path at the CASPT2 level results in a maximum at an H−Co−N angle of 104°, for which a more detailed specification of the geometry can be found in Table 5.

Due to the large distance between the migrating proton H_m and the nitrogen atom in the transition state, there is no longer any interaction between the two atoms. We therefore conclude that TS1 plays a key role in the different experimentally observed reactions. It constitutes a very important point on the potential energy surface. All the reactions that require the breaking of at least one NH bond can pass via a structure in the vicinity of TS1. From this point on, the $[HCoNH_2]^+$ system can proceed in four different ways (Figure 3). First, the breaking of one metal ligand bond will lead to the elimination of a hydrogen atom (reaction 3) or an NH_2 group (reaction 4). Second, the H−Co−N angle can enlarge, to give the $HCoNH_2^+$ inserted complex: reaction 2. Third, a second NH bond can also be activated, leading to H_2 elimination possibly via a second transition state TS2 (reaction 5).

$HCoNH_2^+$. By enlarging the H_m-Co-C angle, from TS1 on, the energy lowers, leading to a stable inserted complex. As was suggested by the experiment, the $HCoNH_2^+$ complex is a local minimum, separated by a barrier from the adduct. Starting from several geometries, the optimizations at the CASSCF level always gave a planar C_{2v} structure. Table 6 contains the geometries of the four different triplet states. The intermediate has a $^3A_1$ ground state. The Co−N distance is about 0.2 Å longer than the Co−N distance in the low-spin $CoNH_2^+$ complex. This is due to the weaker π_{Co-N} bond; the occupation of the π^* orbital in the CASSCF wave functions is about 0.1 electron higher than in the amide complex.

TABLE 6: $HCoNH_2^+$ Insertion Complex: Geometries and Relative Energies with Respect to the Ground State ($^3A_1$) for the Different Low-Lying States

	$^3A_1$	$^3B_1$	$^3B_2$	$^3A_2$
Co−N (Å)	2.10	2.13	2.12	2.10
$Co-H_m$ (Å)	1.63	1.65	1.63	1.63
Co−N−H (deg)	125.9	125.9	126.0	125.9
ΔE (kcal/mol)	0.0	13.1	3.3	1.7

TABLE 7: Geometry of the Transition State for the H_2 Elimination (H_m and H_p Are the Migrating Protons)

Co−N (Å)	1.91
$Co-H_m$ (Å)	1.84
H_p-H_m (Å)	0.99
H_m-Co-N (deg)	74.9
$Co-N-H_p$ (deg)	67.2
$H_m-Co-N-H$ (deg)	176.8

TABLE 8: Relative Energies with Respect to the Ground-State Asymptote (Co^+ (^3F) + NH_3) of the Various Stationary Points on the Potential Energy Surface. Negative Values for ΔE Correspond to Exothermic Reactions

molecule	CASPT2	rel	BSSE	ZPE	ΔE
$CoNH_3^+$	−57.0	−3.5	+5.5	+2.9	−52.1
TS1[a]	9.6	−7.7	+8.2	−2.3	7.8
$HCoNH_2^+$	1.3	−8.5	+8.5	−7.8	−6.5
$CoNH_2^+ + H$	43.5	−8.2	+6.1	−7.2	34.2
$CoH^+ + NH_2$	63.4	−8.5	+3.5	−7.8	50.6
TS2	81.3	−8.0	+7.5	−7.1	73.7(58)[b]
$CoNH^+ + H_2$	34.1	−7.5	+5.1	−10.0	21.7

[a] Transition state localized by performing CASPT2 calculations on the CASSCF reaction path. [b] Double-shell effect cannot be dealt with due to the large active space needed. An estimation of 15 kcal/mol applied (see text).

H_2 Elimination: TS2. By rotating the NH_2 group in the first transition state, a four-center bond can be formed. A localization of the transition state at the CASSCF level gives a structure possessing just one imaginary frequency of 1686i cm^{-1}. The geometry of this structure is given in Table 7. The geometry differs only slightly from C_s symmetry. The H_m-H_p distance is already shortened to 0.99 Å; the Co−N bond length is between the value in $HCoNH_2^+$ (2.10 Å) and $CoNH^+$ (1.68 Å).

It should be noted that for the TS2 no full double-shell effect can be evaluated, because this would take a 14i15 active space, which is too large to handle. For similar structures on the reaction surface, the double-shell effect amounts to about 10 kcal/mol. We can therefore estimate this effect in TS2 to be more or less the same. To be on the safe side with regard to the corresponding energy barrier, we put forward a value of about 15 kcal/mol. The activation energy of 58 kcal/mol should therefore be looked upon as a lower limit. This large value does not come as a surprise: tight four-center transition states were also calculated at high energies for the H_2 elimination reactions of Co^+ and Fe^+ from methane.[5,7] In addition, a previous systematic study for the cations of first-row transition metals[13] showed that the late metal cations are characterized by a high barrier, whereas for the early metal cations a low barrier is predicted. It was argued that the parameter determining the barrier height is the magnitude of the 4s participation in the M^+-L bond. For the late metal cations this participation is high, giving rise to a forbidden $2_s + 2_s$ reaction, whereas for the early metals the 3d involvement in the M−L bonds is larger,

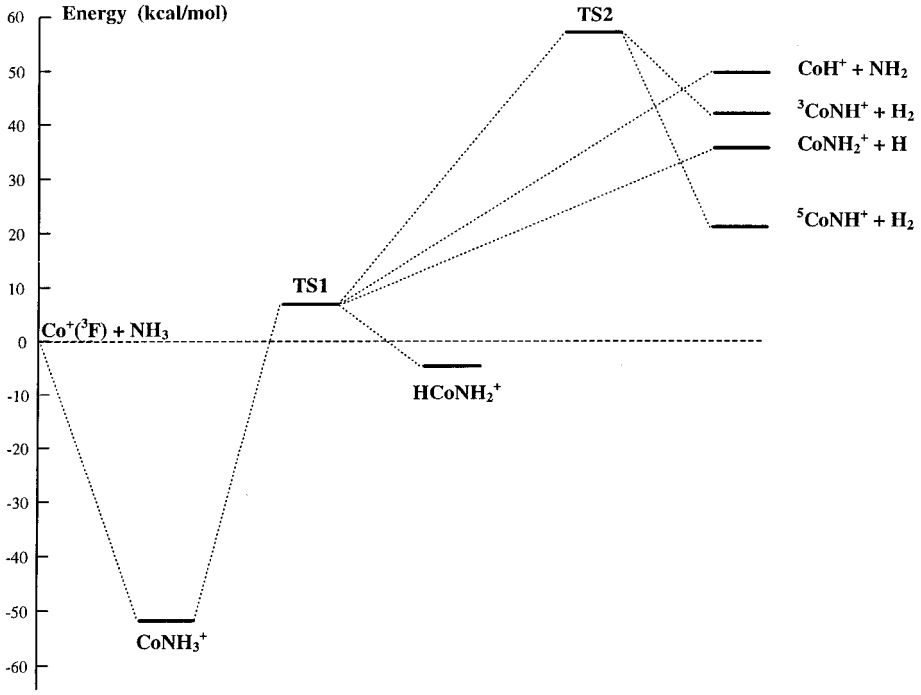

Figure 4. CASPT2 reaction profile for the reaction of Co^+ with ammonia. Exothermic reactions correspond to negative energy values. All structures are positioned with respect to the ground-state asymptote (Co^+ (^3F) + NH_3). $^3CoNH^+$ and $^5CoNH^+$ denote the $^3\Phi$ and $^5\Delta$ structures, respectively, of the $CoNH^+$ ion.

which makes the concerted bond breaking and making more feasible. Again, in the late metal cations the more effective screening of the 3d orbitals by the 4s orbital is responsible for the experimentally observed reactivity across the first row. Indeed, for the reactions of early metal cations with methane and ammonia, H_2 elimination occurs at low kinetic energies.

Comparison with Experiment. The relative energies of all the intermediates, transition states, and exit channels, are given in Table 8 and Figure 4. All the values are corrected for relativistic effects, BSSE, and zero-point vibrational energies. The first conclusion to be drawn from comparison of the different energies is that the $HCoNH_2^+$ structure is indeed found to be a stable intermediate. This insertion complex is situated at about 7 kcal/mol under the asymptotic energy of Co^+ (^3F) and NH_3. Clemmer et al.[21] suggested a thermo-neutral formation. This is essentially confirmed by our calculations, since the CASPT2 bond energies can be assumed to be overestimated by about 5 kcal/mol (due to the improper description of the 4s, 3d promotion energy). The barrier for the reverse reaction (insertion complex to adduct) is about 15 kcal/mol, which is high enough to guarantee its experimentally observed stability. A barrier of 18 kcal/mol was proposed by Clemmer et al.[21] With respect to the entrance channel they suggested an energy barrier of 20 kcal/mol. On the basis of our calculation and taking into account the d^8 to s^1d^7 excitation error, we estimate this barrier to be 10−15 kcal/mol above the ground-state asymptote. If we make a comparison with our previous theoretical study on the isoelectronic $[CoCH_4]^+$ system,[12] the stability of the triplet $HCoNH_2^+$ comes somewhat as a surprise. Indeed, no stationary $HCoCH_3^+$ structure could be located at the CASPT2 level. We ascribe the main reason for the different behavior of the two systems to the availability of the 2p orbital of the NH_2, group which has the capability of stabilizing the insertion product with respect to the transition state. This is witnessed by the planar structure of the $CoNH_2$ moiety in the insertion product, which is the result of a π bond between the sp^2-hybridized NH_2 ligand and Co^+. TS1 has a bent structure, indicating that the π bond has not fully developed at this stage of the insertion process.

A second conclusion we can draw from the relative energies has to do with the reason that reaction 5 is not observed. Figure 4 shows that the dehydrogenation requires a high activation energy of 58 kcal/mol above the entrance channel. The exit channels for NH_2 (reaction 4) and H elimination (reaction 3) are situated at respectively about 8 and 24 kcal/mol below TS2 and at 50.6 and 34.2 kcal/mol above the entrance channel. This means that at low kinetic energies (smaller than 34.2 kcal/mol or 1.5 eV) only the adduct formation (exothermic reaction) and the oxidative insertion into a Co−N bond are possible (activation energy of about 10−15 kcal/mol). If Co^+ is accelerated to higher kinetic energies, first the $CoNH_2^+$ channel and eventually the CoH^+ channel come in reach. Under these circumstances the system is likely to react directly without the formation of the $HCoNH_2^+$ complex as an intermediate. This can be understood from the linear structure of the H_m−Co−N moiety of the intermediate. Well before this intermediate is formed on the reaction surface, the bond between the remaining NH_2 group and the migrating hydrogen is completely broken (even in the TS1 structure). So, at elevated kinetic energies a simple breaking of a single Co^+−N or Co^+−H bond is a more likely process than the formation of an insertion complex or the dehydrogenation through a tight and complex four-center transition state (at energies high enough to reach TS2). This explains that the relative experimental cross sections for both observed elimination channels (CoH^+ and $CoNH_2^+$) point to a direct mechanism without the involvement of an intermediate and why the H_2 elimination is not experimentally observed.[21]

Conclusion

The calculated energetics of the exit channels, as well as the binding energy of the molecular complex, are in reasonable agreement with the experimental values, thereby justifying the theoretical methods used in the present paper. The calculated binding energies for the $CoNH_2^+$ and CoH^+ ions are only slightly overestimated due to the underestimation of the Co^+ ($^3F \rightarrow {}^5F$) excitation energy. At the highest level of theory used,

the $HCoNH^+$ complex is found to be a minimum on the potential energy surface, separated from the adduct by a barrier that is high enough to guarantee a certain lifetime for the intermediate, so as to make it observable. The fact that the H_2 elimination is not observed, even at high entrance energies, is due to the high barrier for this elimination, which is above both the NH_2 and H elimination energies. At high entrance energies, the mechanistically simpler NH_2 or H elimination will always be favored. Differences in stability and geometry between the early metal cation compounds MNH_x^+ ($x = 1, 2$) on one hand and their Co^+ counterparts on the other hand are thought to be the consequence of the trend of the relative radial extension of the 4s and 3d orbitals across the row. The 4s orbital of Co^+ prevents the 3d orbitals from fully participating in the bond formation process.

References and Notes

(1) Eller, K.; Schwarz, H. *Chem. Rev.* **1991**, *91*, 1121.
(2) *Organometallic Ion Chemistry*; Freiser, B. S., Ed.; Kluwer: Dordrecht, 1995.
(3) Weisshaar, J. C. *Gas-Phase Metal Reactions*; Fontijn, A., Ed.; North-Holland: Amsterdam, 1992.
(4) Blomberg, M. R. A.; Siegbahn, P. E. M.; Svenson, M. J. *J. Phys. Chem.* **1994**, *98*, 2062.
(5) Musaev, D. G.; Morokuma, K. *J. Chem. Phys.* **1994**, *101*, 10697.
(6) Haynes, C. L.; Chen Y.-M.; Armentrout, P. B. *J. Phys. Chem.* **1996**, *100*, 111.
(7) Holthausen, M. C.; Fiedler, A.; Schwarz, H.; Koch, W. *J. Phys. Chem.* **1996**, *100*, 6236.
(8) Musaev, D. G.; Morokuma, K; Koga, N.; Nguyen, K. A.; Gordon, M. S.; Cundari, T. R. *J. Phys. Chem.* **1993**, *97*, 11435.
(9) Haynes, C. L.; Chen Y.-M.; Armentrout, P. B. *J. Phys. Chem.* **1995**, *99*, 9110.
(10) Haynes, C. L.; Fisher E. R.; Armentrout, P. B. *J. Am. Chem. Soc.* **1996**, *118*, 3269.
(11) Haynes, C. L.; Fisher E. R.; Armentrout, P. B. *J. Phys. Chem.* **1996**, *100*, 18300
(12) Hendrickx, M.; Ceulemans, M.; Vanquickenborne, L. *Chem. Phys. Lett.* **1996**, *257*, 8.
(13) Hendrickx, M.; Ceulemans, M.; Gong, K.; Vanquickenborne, L. *J. Phys. Chem.* A **1997**, *101*, 2465.
(14) Sunderlin, S. L.; Armentrout, P. B. *J. Am. Chem. Soc.* **1989**, *111*, 3845.
(15) Sunderlin, S. L.; Armentrout, P. B. *J. Phys. Chem.* **1988**, *92*, 1209.
(16) Aristov, N.; Armentrout, P. B. *J. Phys. Chem.* **1987**, *91*, 6178.
(17) Fiedler, A.; Schröder, D.; Shaik, S.; Schwarz, H. *J. Am. Chem. Soc.* **1994**, *116*, 10734.
(18) Shaik, S.; Danovich, D.; Fiedler, A.; Schröder, D.; Schwarz, H. *Helv. Chim. Acta* **1995**, *78*, 1393.
(19) Schröder, D.; Fiedler, A.; Ryan, M. F.; Schwarz, H. *J. Phys. Chem.* **1994**, *98*, 68.
(20) Clemmer, D. E.; Armentrout, P. B. *J. Am. Chem. Soc.* **1989**, *111*, 8280.
(21) Clemmer, D. E.; Armentrout, P. B. *J. Phys. Chem.* **1991**, *95*, 3084.
(22) Clemmer, D. E.; Sunderlin, S. L.; Armentrout, P. B. *J. Phys. Chem.* **1990**, *94*, 3008.
(23) Clemmer, D. E.; Armentrout, P. B. *J. Phys. Chem.* **1990**, *94*, 208.
(24) Andersson, K.; Malmqvist, P.-A.; Roos, B. O.; Sadlej, A. J., Wolinski, K. *J. Phys. Chem.* **1990**, *94*, 5483.
(25) Pou-Amerigo, R.; Merchan, M.; Nebot-Gil, I.; Malmqvist, P.-A.; Roos, B. O. *J. Chem. Phys.* **1994**, *101*, 4893.
(26) Pierloot. K.; Dumez, B.; Widmark, P.-O.; Roos, B. O. *Theor. Chim. Acta* **1995**, *90*, 87.
(27) Schmidt, M. W.; Baldridge, K. K.; Boatz, J. A.; Jensen, J. H.; Koseski, S.; Gordon, M. S.; Nguyen K. A.; Windus, T. L.; Elbert, S. T. *QCPE Bull.* **1990**, *10*, 52.
(28) Persson, B. J.; Roos, B. O.; Pierloot, K. *J. Chem. Phys.* **1994**, *101*, 6810.
(29) *MOLCAS* version 3; Andersson, K., Blomberg, M. R. A., Fulscher, M. P., Kello, V., Lindh, R., Malmqvist, P.-A., Noga, J., Olsen, J., Roos, B. O., Sadlej, A. J., Siegbahn, P. E. M., Urban, M., Widmark, P.-O., Eds.; University of Lund: Sweden 1994.
(30) Langhoff, S. R.; Bauschlicher, C. W.; Partridge, H.; Sodupe, M. *J. Phys. Chem.* **1991**, *95*, 10677.
(31) Haynes, C. L.; Armentrout, P. B.; Perry, J. K.; Goddard, W. A., III *J. Phys. Chem.* **1995**, *99*, 6340.
(32) Mavridis, A.; Herrera, F. L.; Harrison, J. F. *J. Phys. Chem.* **1991**, *95*, 6854.
(33) Kapellos, S.; Mavridis, A.; Harrison, J. F.; Allison, J. *J. Phys. Chem.* **1991**, *95*, 6860.
(34) Bruckner S. W.; Gord, J. R.; Freiser, B. S. *J. Am. Chem. Soc.* **1988**, *110*, 6606.
(35) Cundari, T. R. *J. Am. Chem. Soc.* **1992**, *114*, 7879.
(36) Shilling, J. B.; Goddard, W. A., III; Beauchamp, J. L. *J. Am. Chem. Soc.* **1986**, *108*, 582.
(37) Petterson, L. G. M.; Bauschlicher, C. W.; Langhoff, S. R. Partridge, H. *J. Chem. Phys.* **1987**, *87*, 481.
(38) Elkind, J. L.; Armentrout, P. B. *J. Phys. Chem.* **1986**, *90*, 576.
(39) Pierloot, K.; Tsokos, E.; Roos, B. O. *Chem. Phys. Lett.* **1993**, *214*, 583
(40) Martin, R. L. *J. Phys. Chem.* **1983**, *87*, 750.